Reports of Practical Oncology and Radiotherapy 25 (2020) 703–708

Available online at www.sciencedirect.com

Reports of Practical Oncology and Radiotherapy

journal homepage: http://www.elsevier.com/locate/rpor

Original research article

Dosimetric impact of baseline drift in volumetric modulated arc therapy with breath holding

Shunsuke Ono, Yoshihiro Ueda*, Shoki Inui, Masaru Isono, Shingo Ohira, Seiya Murata, Masayoshi Miyazaki, Teruki Teshima

Department of Radiation Oncology, Osaka International Cancer Institute, 3-1-69 Otemae, Chuou-ku, Osaka, 537-8567, Japan

ARTICLE INFO

Article history:
Received 11 December 2019
Received in revised form 17 April 2020
Accepted 1 June 2020
Available online 8 June 2020

Keywords:
Breath holding
Volumetric modulated arc therapy
Baseline drift
Dosimetry
Pancreatic cancer

ABSTRACT

Background: We investigated the change of dose distributions in volumetric modulated arc therapy (VMAT) under baseline drift (BD) during breath holding.
Materials and methods: Ten VMAT plans recalculated to a static field at a gantry angle of 0° were prepared for measurement with a 2D array device and five original VMAT plans were prepared for measurement with gafchromic films. These measurement approaches were driven by a waveform reproducing breath holding with BD. We considered breath holding times of 15 and 10 s, and BD at four speeds; specifically, BD0 (0 mm/s), BD0.2 (0.2 mm/s), BD0.3 (0.3 mm/s), and BD0.4 (0.4 mm/s). The BD was periodically reproduced from the isocenter along the craniocaudal direction and the shift during breath holding ($Shift_{BH}$) ranged 0–6 mm.

The dose distribution of BD0.2, BD0.3 and BD0.4 were compared to that of BD0 using gamma analysis with the criterion of 2%/2 mm.
Results: The mean pass rates of each $Shift_{BH}$ were 99.8% and 98.9% at 0 mm, 96.8% and 99.4% at 2 mm, 94.9% and 98.6% at 3 mm, 91.5% and 98.4% at 4 mm, 70.8% and 94.1% at 4.5 mm, and 55.0% and 83.6% at 6 mm for the array and film measurements, respectively.
Conclusion: We found significant differences in $Shift_{BH}$ above 4 mm ($\rho < 0.05$). Hence, it is recommended that breath holding time should be shortened for patients to preserve the reproducibility of dose distributions.

1. Introduction

In radiotherapy for pancreatic tumors, organs at risk surrounding the pancreas have strict dose constraints.[1] In addition, for chest or abdominal regions, which present respiratory motion, the standard is to define internal target volumes to prevent geometric errors induced by this motion.[2] However, considerable respiratory motion expands the internal target volume and, consequently, the radiation fields, thus hindering the delivery of sufficient radiation dose to the tumors.[3]

To concentrate the appropriate dose to pancreatic tumors and spare organs at risk, volumetric modulated arc therapy (VMAT) rotating the gantry and modulating the intensity of the radiation dose with a multi-leaf collimator (MLC) was an effective technique.[4] In addition, the breath holding (BH) technique was recommended to prevent expanding the radiation field due to respiratory motion.[5] In clinical practice, the respiratory-gated and BH techniques with several guidance systems using external surrogates have been widely used.[6,7] Radiotherapy with BH directly reduces respiratory motion of tumors, reducing the treatment time and increasing its effectiveness.[8] Hence, VMAT with BH (BH-VMAT) effectively concentrates the dose to pancreatic tumors.

However, there are still variations in abdominal motion by pulsation of the aorta and baseline drift (BD) of tumors during BH. Although BH is focused on the moving target, the target position may not always remain steady.[9,10] In addition, VMAT is susceptible to dose variation from the interplay between the MLC sequence and tumor motion. Consequently, hot and cold spots of radiation dose inside the target can occur.[11] Although a BD from 0 to 6 mm can reduce the reproducibility of dose distribution during intensity-modulated radiation therapy,[12] scarce research on the effect of BD in BH-VMAT is available. In this study, we assessed the dosimetric impact of BD in BH-VMAT for pancreatic cancer in a phantom study.

* Corresponding author.
E-mail address: ueda-yo@mc.pref.osaka.jp (Y. Ueda).

https://doi.org/10.1016/j.rpor.2020.06.004
1507-1367/

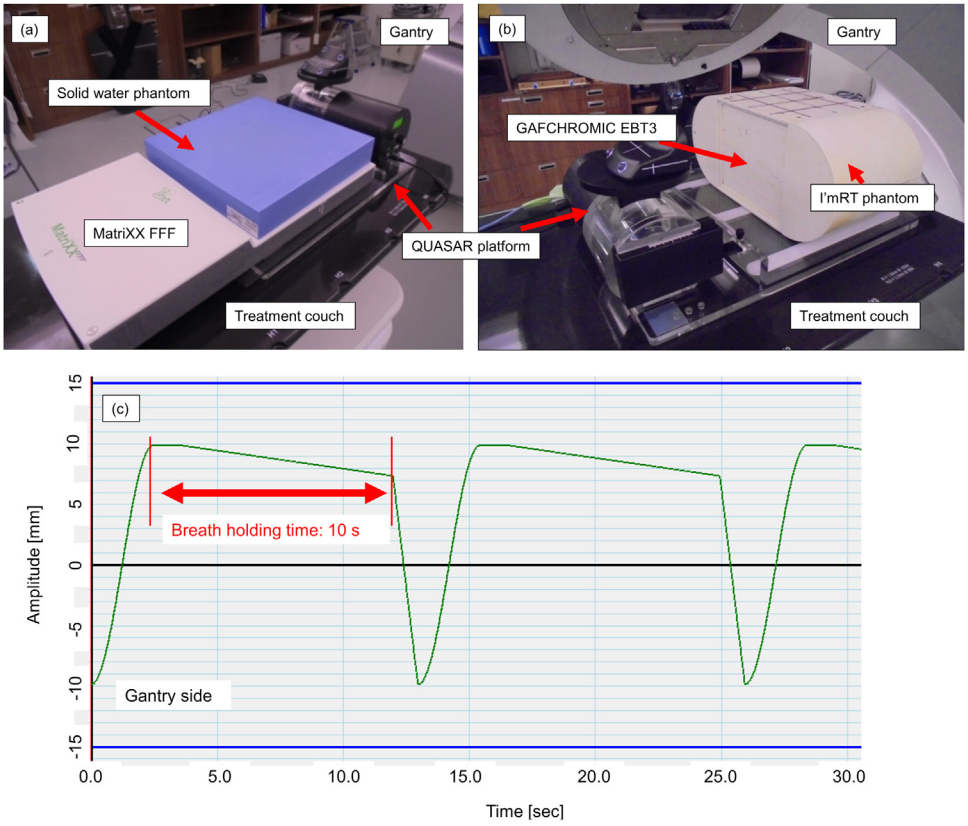

Fig. 1. (a) MatriXX measurement setup. MatriXX on QUASAR Respiratory Motion Platform and placed on treatment couch. A solid water phantom of $30 \times 30 \times 5\,cm^3$ was placed on MatriXX. (b) Film measurement setup. I'mRT phantom on QUASAR platform and placed on treatment couch. EBT3 was inserted horizontally at the center of I'mRT phantom. (c) Waveform for baseline drift of 0.3 mm/s to move QUASAR platform. The green line indicates the waveform, and each red line represents the start and end of breath holding. The interval between red lines corresponds to the breath holding time. Each device was held at opposite gantry sides during breath holding repeatedly (For interpretation of the references to colour in this figure legend, the reader is referred to the web version of this article).

2. Materials and methods

2.1. Subjects and CT simulation

Ten patients with inoperable pancreatic cancer undergoing VMAT treatment at the Osaka International Cancer Institute between September 2017 and August 2018 were enrolled in this study.

For CT simulation and treatment, each patient was immobilized with a vacuum cushion. CT scanning was performed by multi-slice CT (RevolutionHD; GE Medical Systems, Milwaukee, WI, USA) with 2 mm slice thickness, 512×512 matrix size, and 50 cm field of view during exhalation and inspiration. Additionally, 4D-CT scans were obtained from the Real-time Position Management system (Varian Medical Systems, Palo Alto, CA, USA) by placing its marker on patients' abdomen. The breathing signal and acquired CT images were transferred to the Advantage Sim Workstation (GE Medical Systems). Average intensity projection and maximum intensity projection CT image sets were created from 10 phase CT images.

2.2. Treatment planning

The 10 phase CT images, average intensity projection images, and maximum intensity projection images were transferred to a treatment planning system (Eclipse; Varian Medical Systems). The clinical target volume covered the celiac artery, superior mesenteric artery, and para-aortic lymph node regions, and it was contoured on each phase CT image. The internal target volume was combined from clinical target volumes on each phase CT image. The planning target volume (PTV) was created by adding 5 mm margins to the internal target volume.[13] Organs at risk were contoured on the average intensity projection images. The prescribed dose was 50.4 Gy in 28 fractions at the mean dose for the PTV. Dose limitations in organs at risk for V_{50} (absolute volume receiving doses in excess of 50 Gy) at the duodenum and stomach were below 15 cm^3, and for V_{18} (volume ratio receiving doses in excess of 18 Gy) at the kidneys below 20%.[14–16]

The treatment plan was designed on the TrueBeam STx treatment system (Varian Medical Systems), which contains a high-definition MLC with 2.5 mm leaf width at the isocenter. The plans have one or two arc fields with collimator angles of $\pm 20^\circ$ or $\pm 30^\circ$. For the beam parameters, the energy and maximum dose rate were 6 MV and 600 MU/min, respectively. The optimization and calculation algorithms were Photon Optimizer ver. 13.0 and Analytical Anisotropic Algorithm ver. 13.0 (Varian Medical Systems). The grid sizes of the optimization and dose calculations were 2.5 and 2.0 mm, respectively.

2.3. Modulation complexity score for VMAT

The modulation complexity score for VMAT (MCSv), which indicates the modulation degree of the MLC leaves of a VMAT plan was calculated using our in-house software implemented on MATLAB R2016a (MathWorks, Natick, MA, USA) for each arc field. The MCSv has values ranging from 0 to 1, where values close to zero indicate that the MLC motion is highly complex,[17] and it is obtained from the leaf sequence variability, aperture area variability, and normalized monitor-unit value.[18,19] The detailed parameters of each plan are listed in Table 1.

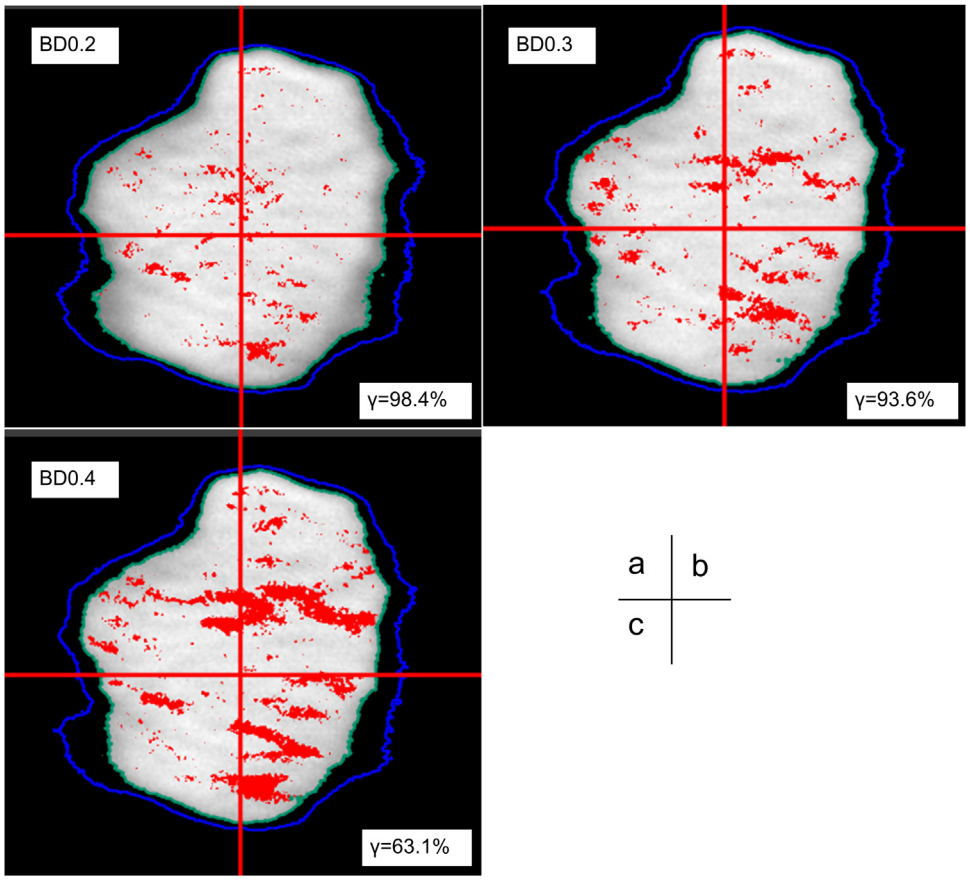

Fig. 2. Dose distributions of coronal images for baseline drifts of (a) 0.2 (BD0.2), (b) 0.3 (BD0.3) and (c) 0.4 mm/s (BD0.4) were compared with that for baseline drift of 0 mm/s using gamma analysis with the criterion of 2%/2 mm (threshold 50%) during film measurement. The intersection of two red lines indicates the isocenter. The light green and blue lines indicate the 50% and 30% isodose contours, respectively. Each red dot represents a region with gamma >1 (For interpretation of the references to colour in this figure legend, the reader is referred to the web version of this article).

Table 1
Treatment parameters for each patient including planning target volume (PTV), monitor units (MU), leaf sequence variability (LSV), aperture area variability (AAV), and modulation complexity score for VMAT (MCSv).

Patient	PTV [cm^3]	MU	LSV	AAV	MCSv
1	150.3	592	0.707	0.407	0.284
2	70.7	410	0.705	0.518	0.369
3	162.7	517	0.718	0.453	0.331
4	152.2	553	0.714	0.474	0.335
5	81.5	553	0.687	0.516	0.357
6	313.2	310	0.796	0.601	0.474
7	110.4	476	0.717	0.567	0.403
8	85.3	598	0.683	0.485	0.331
9	193.1	457	0.724	0.517	0.373
10	28.9	426	0.654	0.488	0.316

2.4. Measurements

Two phantoms were prepared on the QUASAR Respiratory Motion Platform (Modus Medical Devices, London, ON, Canada). First, the MatriXX FFF detector (IBA Dosimetry, Schwarzenbruck, Germany) was set as shown in Fig. 1a (SCD: source chamber distance = 100 cm). A solid water phantom (Gammex, Middleton, WI, USA) of $30 \times 30 \times 5\,cm^3$ was placed on the MatriXX FFF. The spatial resolution of the MatriXX FFF, pixel size of 7.62 mm center-to-center, chamber volume of 32 mm^3, was limited by the center-to-center distance between the ion chambers.[20] Then, I'mRT phantom (IBA Dosimetry) and Gafchromic EBT3 (International Specialty Products, Wayne, NJ) were prepared. Gafchromic EBT3 film was introduced to eliminate measurement orientation effects and has been used most commonly for dose analysis.[21] EBT3 was inserted horizontally at the center of I'mRT phantom to detect coronal dose distributions at the center (Fig. 1b). CT images of these phantoms were acquired using matrix size of 512×512, field of view of 50 cm, and slice thickness of 2.0 mm. Ten clinical plans were recalculated as verification plans on the CT images for the MatriXX FFF detector with a fixed field at a gantry angle of 0°. In each verification plan, the isocenter was set at the center of chambers arranged regularly in the MatriXX FFF detector (SCD = 100 cm). In addition, five clinical plans were recalculated as verification plans on the CT images for the I'mRT phantom. The isocenter corresponded with the center of the film inserted into the phantom.

In film measurements, arc fields were the same as those used in clinical plans. Measurements were combined with the Real-time Position Management system to perform gated irradiation. During irradiation of the verification plans, each phantom moved in the craniocaudal direction from head to feet by a waveform reproducing BH using the QUASAR Respiratory Motion Platform. Four BH patterns at BD speeds BD0 (0 mm/s), BD0.2 (0.2 mm/s), BD0.3 (0.3 mm/s), and BD0.4 (0.4 mm/s) were prepared. In addition, two BH times were evaluated, namely, BH15 (15 s) and BH10 (10 s). Fig. 1c shows the waveform combining speed BD0.3 and BH10. The top part of the waveform agrees with the isocenter. Baseline drift was reproduced to move from the isocenter.

For film measurement, the irradiated films were scanned using the Epson Scan software (Epson, Nagano, Japan) and a calibration

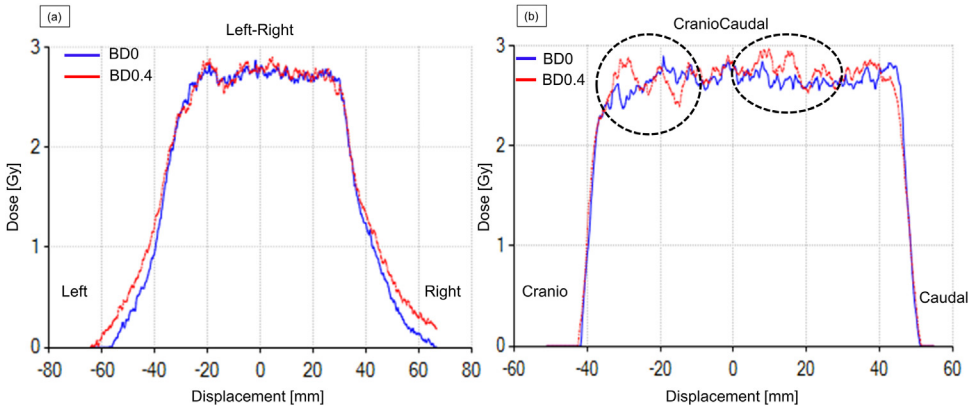

Fig. 3. Dose profiles at isocenter along the (a) left–right and (b) craniocaudal directions for the lowest pass rate during film measurement. The blue and red lines represent baseline drift of 0 (BD0) and 0.4 mm/s (BD0.4), respectively. The dotted circles represent regions with large differences between BD0 and BD0.4 (For interpretation of the references to colour in this figure legend, the reader is referred to the web version of this article).

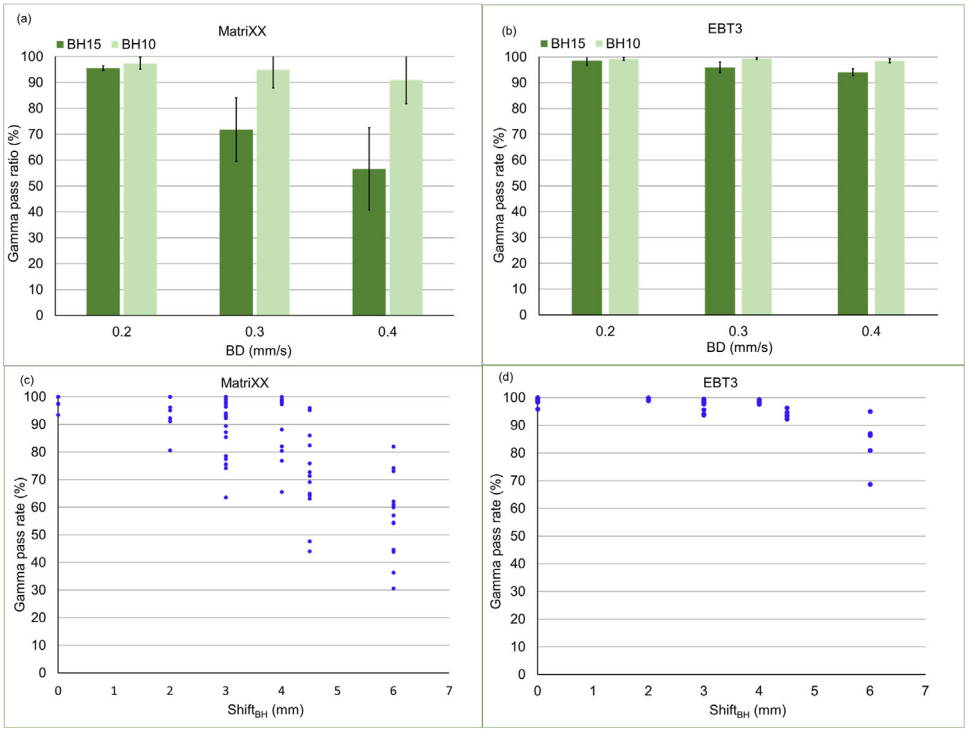

Fig. 4. Mean and standard deviation of the γ pass rate per baseline drift (BD) speed during (a) MatriXX and (b) film measurements. Dark and light green shades represent breath holding times of 15 and 10 s. Relationship between the γ pass rate and BD during (c) MatriXX (d) film measurements (BH, breadth holding time) (For interpretation of the references to colour in this figure legend, the reader is referred to the web version of this article).

curve was acquired to convert the films into dose data. The dose distribution on the film was normalized at the center dose. Each dose distribution was analyzed using the Akilles software suite (RADLab, Osaka, Japan).

2.5. Data analysis

For both measurements, the dose distribution for BD0 was compared to that for no-gating to verify the system performance. Next, the dose distributions at each BD speed (i.e., BD0.2, BD0.3, and BD0.4) were compared with the distribution for BD0. For planar dose comparision gamma evaluation, the γ technique was used. The γ index technique calculates quantity γ for each point of the region of interest (ROI) using dose difference (DD) and distance-to-agreement (DTA) criterion of 2%/2 mm.[22] ROI was set to area receiving more than 50% isodose to target. Moreover, the shift during BH time ($Shift_{BH}$) was calculated as

$$Shift_{BH} = BDSpeed \times BHTime.$$

Thus, $Shift_{BH}$ ranged from 0 to 6 mm per BD, and we obtained the relation between the γ pass rate and $Shift_{BH}$. A paired Student's *t*-test was used to determine significant differences at each BD, with values of $\rho < 0.05$ indicating statistical significance.

3. Results

The means ± standard deviations of the pass rate between the non-gated VMAT and BD0 were 99.4 ± 0.63% and 99.8 ± 1.71% for BH15 and BH10 during the MatriXX measurement, respectively, and 98.5 ± 1.68% and 99.3 ± 0.61% for BH15 and BH10 during

the film measurement, respectively. Hence, there is a negligible mechanical error in the dose distributions when using the gating system.

Fig. 2 shows the dose distributions for BD0.2, BD0.3 and BD0.4 compared to BD0 at BH15 during film measurement. The errors for BD0.3 and BD0.4 are clearly larger than the error of BD0.2, with the highest failing percentage of the γ pass rate reaching 36.9% for BD0.4.

Fig. 3 shows the dose profiles at the isocenter between BD0 and driven BD0.4 obtained from patient 2. There was a relatively large effect along the craniocaudal direction (shown with dotted circles) compared with the left–right direction, because the target moved along the former direction as the diaphragm lowers during BH.

Fig. 4a and b shows the results at each BD speed. For the MatriXX measurement, the mean pass rate of BD0.4 at BH15 decreased largely, but the mean pass rate at BH10 was above the 90% for the criterion of 2%/2 mm. The mean pass rates of BD0.4 and BD0.3 were 57.6 and 72.3% at BH15, respectively, but they were 90.5 and 95.3% at BH10. For the film measurement, the mean pass rate was lower at BH15 than at BH10 for any BD speed. Although there was no statistic difference between BH15 and BH10 for BD0.2 ($\rho > 0.05$), the pass rate at BH15 was statistically lower than that at BH10 for BD0.3 and BD0.4 ($\rho < 0.05$) in both measurements.

Figs. 4c and d show the relations between $Shift_{BH}$ and the γ pass rate. The mean pass rates were 99.8 and 98.9% ($Shift_{BH}$ = 0 mm), 97.5 and 99.4% ($Shift_{BH}$ = 2 mm), 89.6 and 98.6% ($Shift_{BH}$ = 3 mm), 90.9 and 98.4% ($Shift_{BH}$ = 4 mm), 71.1 and 94.1% ($Shift_{BH}$ = 4.5 mm), and 56.4 and 83.6% ($Shift_{BH}$ = 6 mm) for the MatriXX and film measurements, respectively. In both measurements, there were significant differences for BD above 4 mm ($\rho < 0.05$). The correlation values between the γ pass rate and MCSv (0.284–0.474) ranged from 0.03 to 0.120 in each $Shift_{BH}$. There was no correlation between the γ pass rate and MCSv.

4. Discussion

In this study, we investigated the effect of $Shift_{BH}$ for dose distributions in BH-VMAT under two BH times, because it has not been evaluated before. We found that an increasing error for dose distribution in BH-VMAT is not related to the MLC width and suggest a preferable BH time to reduce $Shift_{BH}$.

Two measurement types were evaluated, namely, MatriXX and EBT3, and we determined that the γ pass rate reduction differs between measurements. In general, the spatial resolution of multi-dimensional detectors is lower than that of films.[20] It is also difficult to compare the dose difference at the regions where detectors are not arrayed in multiple dimensions, and there is uncertainty as to when dosimetry measurements are performed.[23] Consequently, it is thought that the pass rate of MatriXX measurements is lower than that of film measurements.

When $Shift_{BH}$ above 4 mm was observed during BH, the γ pass rate was less than 95% for both measurements. Nakamura et al.[12] reported that BD above 5 mm is the cutoff point by the drift being beyond the MLC leaf width at the isocenter level, and BD below 5 mm is preferable to achieve more conformal dose distributions in BH intensity-modulated radiation therapy. The TrueBeam STx treatment system has a high-definition MLC with a minimum leaf width of 2.5 mm and, thus, the cutoff point may be lower than that reported in Ref. 12. During VMAT, the collimator usually rotates, and the cutoff point of BD may not be equal to the MLC leaf width by this rotation. We found no relation between $Shift_{BH}$ and the MLC leaf width in BH-VMAT, and we found a suitable value of $Shift_{BH}$ to be below 4 mm during BH-VMAT. BH times of 10–15 s are generally used in radiotherapy,[24] and a short BH time is preferable to maintain $Shift_{BH}$ in the suggested value. Thus, we recommend a BH time of 10 s for BH-VMAT.

In addition, there was no correlation between the γ pass rate and MCSv. Although VMAT plans retrieve a variety of MLC motions, we investigated the effect of dose distribution by BD, which resulted independent of MCSv. Likewise, no relation was found between the γ pass rate and both the monitor units (310–598) and PTVs (28.9–313.2 cm^3). The effects of dosimetry driven BD were mainly dependent on the BD value.

In general, when respiration-gated radiotherapy is combined with the Real-time Position Management system, an external marker is placed on the patient's body to monitor respiratory motion and acquire the respiration waveform. However, motion of implanted fiducial markers and external markers placed on the patients do not necessarily agree, and these cases should be handled by other methods.[25] In fact, unnoticeable BD during irradiation may occur in such cases, and shortening the BH time can reduce the BD effects.

As a limitation of this study, we only examined intra-fractional but not inter-fractional setup errors. For comparing dose distributions with and without BD, we assumed no setup error in the initial target position. Thus, the observed error in this study can increase under setup errors which are always present in practice. To reduce dose distribution errors induced by BD and setup errors, it is important to reduce BD errors.

The evaluation by Nakamura et al.[12] of the BD effect for intensity-modulated radiation therapy at two BD speeds and our study that evaluated dose distributions at four BD speeds and two BH times for BH-VMAT provide representative data for other related analyses.

5. Conclusion

We investigated the dosimetric impact of BD in BH-VMAT for pancreatic cancer using two measurement approaches, namely array detectors and films. The shift during BH, $Shift_{BH}$, above 4 mm largely reduced the γ pass rate in the PTV. Hence, we recommend that $Shift_{BH}$ should be reduced to below 4 mm, and the BH time should be below 10 s for BH-VMAT, as it is not necessary to further extend the BH time regarding the dose distribution with BD.

Conflict of interest

None declared.

Financial disclosure

This study was supported by JSPS KAKENHI Grant (17K15817) to Yoshihiro Ueda.

Acknowledgements

We would like to thank Editage (www.editage.com) for English language editing.

References

1. Loehrer P, Powell M, Cardenes H, et al. A randomized phase III study of gemcitabine in combination with radiation therapy versus gemcitabine alone in patients with localized, unresectable pancreatic cancer. *J Clin Oncol*. 2008;26:4506.
2. Bussels B, Goethals L, Feron M, et al. Respiration-induced movement of the upper abdominal organs: a pitfall for the three-dimensional conformal radiation treatment of pancreatic cancer. *Radiother Oncol*. 2003;68(1):69–74.
3. Jiang SB. Radiotherapy of mobile tumors. *Semin Radiat Oncol*. 2006;16(4):239–248.

4. Chapman KL, Witek ME, Chen H, Showalter TN, Bar-Ad V, Harrison AS. Pancreatic cancer planning: complex conformal vs modulated therapies. *Med Dosim*. 2016;41(2):100–104.
5. Keall PJ, Mageras GS, Balter JM, et al. The management of respiratory motion in radiation oncology report of AAPM Task Group 76. *Med Phys*. 2006;33(10):3874–3900.
6. Berson AM, Emery R, Rodriguez L, et al. Clinical experience using respiratory gated radiation therapy: comparison of free-breathing and breath-hold techniques. *Int J Radiat Oncol Biol Phys*. 2004;60(2):419–426.
7. Ford EC, Mageras GS, Yorke E, Rosenzweig KE, Wagman R, Ling CC. Evaluation of respiratory movement during gated radiotherapy using film and electronic portal imaging. *Int J Radiat Oncol Biol Phys*. 2002;52(2):522–531.
8. Giraud P, Reboul F, Clippe S, et al. Respiration-gated radiotherapy: current techniques and potential benefits. *Cancer Radiother*. 2003;1:15–25.
9. Nakamura M, Shibuya K, Shiinoki T, et al. Positional reproducibility of pancreatic tumors under end-exhalation breath-hold conditions using a visual feedback technique. *Int J Radiat Oncol Biol Phys*. 2011;79(5):1565–1571.
10. Kim T, Kim S, Park YK, Youn KK, Keall P, Lee R. Motion management within two respiratory-gating windows: feasibility study of dual quasi-breath hold technique in gated medical procedures. *Phys Med Biol*. 2014;59(21):6583–6594.
11. Bortfeld T, Jokivarsi K, Goitein M, Kung J, Jiang SB. Effects of intra-fraction motion on IMRT dose delivery: statistical analysis and simulation. *Phys Med Biol*. 2002;47(13):2203–2220.
12. Nakamura M, Kishimoto S, Iwamura K, et al. Dosimetric investigation of breath-hold intensity-modulated radiotherapy for pancreatic cancer. *Med Phys*. 2012;39(1):48–54.
13. Chavaudra J, Bridier A. Definition of volumes in external radiotherapy: ICRU reports 50 and 62. *Cancer Radiother*. 2001;5(October (5)):472–478.
14. Cassady JR. Clinical radiation nephropathy. *Int J Radiat Oncol Biol Phys*. 1995;31:1249–1256.
15. Jansen EPM, Saunders MP, Boot H, et al. Prospective study on late renal toxicity following postoperative chemoradiotherapy in gastric cancer. *Int J Radiat Oncol Biol Phys*. 2007;67:781–785.
16. Verma J, Sulman EP, Jhingran A, et al. Dosimetric predictors of duodenal toxicity after intensity modulated radiation therapy for treatment of the para-aortic nodes in gynecologic cancer. *Int J Radiat Oncol Biol Phys*. 2014;88(2):357–362.
17. Xu Z, Wang IZ, Kumaraswmy LK, Podgorsak MB. Evaluation of dosimetric effect caused by slowing with multi-leaf collimator (MLC) leaves for volumetric modulated arc therapy (VMAT). *Radiol Oncol*. 2015;50(1):121–128.
18. Masi L, Doro R, Favuzza V, Cipresssi S, Livi L. Impact of plan parameters on the dosimetric accuracy of volumetric modulated arc therapy. *Med Phys*. 2013;40(7):071718.
19. Ohira S, Ueda Y, Isono M, et al. Can clinically relevant dose errors in patient anatomy be detected by gamma passing rate or modulation complexity score in volumetric modulated arc therapy for intracranial tumors? *J Radiat Res*. 2017;58(5):685–692.
20. Wen N, Lu S, Kim J, et al. Precise film dosimetry for stereotactic radiosurgery and stereotactic body radiotherapy quality assurance using Gafchromic™ EBT3 films. *Radiat Oncol*. 2016;11(October (1)):132.
21. Sorriaux J, Kacperek A, Rossomme S, et al. Evaluation of gafchromic(R) EBT3 films characteristics in therapy photon, electron and proton beams. *Phys Med*. 2013;29:599–606.
22. Low DA, Dempsey JF. Evaluation of the gamma dose distribution comparison method. *Med Phys*. 2003;30:2455–2464.
23. Hussein M, Tsang Y, Thomas RA, et al. A methodology for dosimetry audit of rotational radiotherapy using a commercial detector array. *Radioter Oncol*. 2013;108(1):78–85.
24. Tibdewal A, Munshi A, Pathak R, et al. Breath-holding times in various phases of respiration and effect of respiratory training in lung cancer patients. *J Med Imaging Radiat Oncol*. 2015;59(4):520–526.
25. Beddar AS1, Kainz K, Briere TM, et al. Correlation between internal fiducial tumor motion and external marker motion for liver tumors imaged with 4D-CT. *Int J Radiat Oncol Biol Phys*. 2007;67(2):630–638.